Electronic Structure Differences in ZrO 2 vs HfO 2 †

ARTICLE *in* THE JOURNAL OF PHYSICAL CHEMISTRY A · JANUARY 2006

Impact Factor: 2.69 · DOI: 10.1021/jp053593e · Source: PubMed

Electronic Structure Differences in ZrO_2 vs HfO_2†

Weijun Zheng and Kit H. Bowen, Jr.*

Departments of Chemistry and Materials Science, Johns Hopkins University, Baltimore, Maryland 21218

Jun Li,‡ Iwona Dąbkowska,§ and Maciej Gutowski*,§,#

W. R. Wiley Environmental Molecular Sciences Laboratory, Pacific Northwest National Laboratory, Richland, Washington 99352, Department of Chemistry, University of Gdańsk, 80-952 Gdańsk, Poland, and Chemical Sciences Division, Pacific Northwest National Laboratory, Richland, Washington 99352

Received: June 30, 2005; In Final Form: October 18, 2005

Although ZrO_2 and HfO_2 are, for the most part, quite similar chemically, subtle differences in their electronic structures appear to be responsible for differing MO_2/Si (M = Zr, Hf) interface stabilities. To shed light on the electronic structure differences between ZrO_2 and HfO_2, we have conducted joint experimental and theoretical studies. Because molecular electron affinities are a sensitive probe of electronic structure, we have measured them by conducting photoelectron spectroscopic experiments on ZrO_2^- and HfO_2^-. The adiabatic electron affinity of HfO_2 was determined to be 2.14 ± 0.03 eV, and that of ZrO_2 was determined to be 1.64 ± 0.03 eV. Concurrently, advanced electronic structure calculations were conducted to determine electron affinities, vibrational frequencies, and geometries of these systems. The calculated CCSD(T) electron affinities of HfO_2 and ZrO_2 were found to be 2.05 and 1.62 eV, respectively. The molecular results confirm earlier predictions from solid state calculations that HfO_2 is more ionic than ZrO_2. The excess electron in MO_2^- occupies an sd-type hybrid orbital localized on the M atom (M = Zr, Hf). The structural parameters of ZrO_2 and HfO_2 and their vibrational frequencies were found to be very similar. Upon the excess electron attachment, the M−O bond length increases by ca. 0.04 Å, the OMO angle increases by 2−4°, and frequencies of all vibrational modes become smaller, with the stretching modes being shifted by 30−50 cm^{-1} and the bending mode by 15−25 cm^{-1}. Together, these studies unveil significant differences in the electronic structures of ZrO_2 and HfO_2 but not in their structural or vibrational characteristics.

Introduction

Zirconia (ZrO_2) and hafnia (HfO_2) are important materials due to their present and potential future applications in microelectronics,[1−4] catalysis,[5−7] and ceramics.[8−11] Zirconium ($[Kr]4d^25s^2$) and hafnium ($[Xe]4f^{14}5d^26s^2$) reside in the same group of the periodic table, with the most obvious electronic structure difference between them being that hafnium possesses a closed subshell of f-electrons and zirconium has no f-electrons. Also, as a result of ensuing lanthanide contraction,[12] both the atomic and the ionic radii of these atoms are nearly the same. As a result of these similarities, Cotton et al.[12] state "The chemistries of hafnium and zirconium are more nearly identical than for any other two congeneric elements." Indeed, infrared spectra,[13] microwave spectra,[14,15] and theoretical calculations[13−15] show that the vibrational frequencies of molecular ZrO_2 and HfO_2 are quite close in value, and their bond lengths and bond angles are very similar. This is a manifestation of the well-known chemical similarity of Zr and Hf, which is exemplified in their geochemistry: Hf is found in all zirconium minerals and the separation of the two elements is difficult.[12]

Nevertheless, in the solid state, differences emerge between ZrO_2 and HfO_2. For example, significant differences in elastic behavior and transition pressures were suggested for ZrO_2 and HfO_2,[16] and the temperature-induced monoclinic to tetragonal transition is about 500 K higher in HfO_2 than in ZrO_2.[17] Moreover, recent theoretical and experimental work[18] found that the thermodynamic stabilities of ZrO_2 and HfO_2 films are quite different when they are in contact with silicon. In fact, of substantial practical interest, the same study indicates that the HfO_2/Si interface is stable with respect to silicide formation, whereas the ZrO_2/Si interface is not, making HfO_2 a contender as a replacement for SiO_2 as a high-*k* gate dielectric.[18] Because thermodynamic stability is a critical property for microelectronic devices, it is important to better understand the source of the difference. Given that most structural properties of ZrO_2 and HfO_2 are very similar, differences between their solid state properties must trace back to subtle differences in electronic structure. The difference between adiabatic electron affinities of otherwise similar molecules provides a sensitive measure of their electronic structure differences. To determine these values experimentally, we measured the gas phase, anion photoelectron spectra of ZrO_2^- and HfO_2^-, whereas to obtain them theoretically, we conducted electronic structure calculations on MO_2 and MO_2^- (M = Zr, Hf) using density functional theory (DFT) and wave function-theory-based ab initio methods.

Molecular ZrO_2 and HfO_2 were previously reported as polar structures.[13−15,19] The results of a matrix isolation study indicated

† Part of the special issue "Jack Simons Festschrift".

* Corresponding authors. E-mail: K.H.B., kbowen@jhu.edu; M.G., maciej.gutowski@pnl.gov.

‡ W. R. Wiley Environmental Molecular Sciences Laboratory, Pacific Northwest National Laboratory.

§ University of Gdańsk.

Chemical Sciences Division, Pacific Northwest National Laboratory.

10.1021/jp053593e CCC: $30.25
Published on Web 11/16/2005

TABLE 1: Experimental Electron Affinities and Vibration Frequencies for TiO_2, ZrO_2, and HfO_2[a]

	adiabatic electron affinity	vib freq from PES	vib freq from matrix IR[b]
TiO_2	1.59 ± 0.03 eV[c]	940 ± 40 cm^{-1} (υ_1)[c]	946.9 cm^{-1} (υ_1), 917.1 cm^{-1} (υ_3)
ZrO_2	1.64 ± 0.03 eV[d]	887 ± 40 cm^{-1} (υ_1)[d]	884.3 cm^{-1} (υ_1), 818.0 cm^{-1} (υ_3)
HfO_2	2.14 ± 0.03 eV[d]	887 ± 40 cm^{-1} (υ_1)[d]	883.4 cm^{-1} (υ_1), 814.0 cm^{-1} (υ_3)

[a] υ_1 symmetric stretching, υ_3 asymmetrical stretching, υ_2 bending, υ_2 is not shown here. [b] Reference 13. [c] Reference 38. [d] This PES experiment.

that the MO_2 (M = Zr, Hf) is bent, and the upper limit for $\angle$OMO was assigned to $113 \pm 5°$ and $115 \pm 5°$ for M = Zr and Hf, respectively.[13] The stretching frequencies of these C_{2v} structures are strikingly similar: $\upsilon_1(a_1) = 884.3$ and 883.4 cm^{-1}, $\upsilon_3(b_2) = 818$ and 814 cm^{-1}, for ZrO_2 and HfO_2, respectively; see also Table 1.[13] More accurate structures were determined from rotational spectra: the Zr−O bond length is 1.7710 ± 0.0007 Å, $\angle$OZrO = $108.11 \pm 0.08°$,[14] the Hf−O bond length is 1.7764 ± 0.0004 Å, $\angle$OHfO = $107.51 \pm 0.01°$.[15] The electric dipole moments determined from Stark-effect measurements are 7.80 and 7.92 D for ZrO_2 and HfO_2, respectively.[13,14] Finally, the frequency of the bending vibration of ZrO_2 was estimated to be 290 cm^{-1}, on the basis of its inertial defect.[14]

Methods

Experimental Methods. Anion photoelectron spectroscopy is conducted by crossing a mass-selected beam of negative ions with a fixed-frequency laser beam and energy-analyzing the resultant photodetached electrons. The technique is governed by the following energy-conserving relationship:

$$h\upsilon = \mathrm{EKE} + \mathrm{EBE} \quad (1)$$

where $h\upsilon$ is the photon energy, EKE is the measured electron kinetic energy, and EBE is the electron binding energy. The experiment was conducted on an apparatus consisting of a Nd:YAG laser vaporization source, a linear time-of-flight mass spectrometer, a mass gate, a momentum decelerator, a second Nd:YAG laser, and a magnetic bottle energy analyzer. The resolution of our magnetic bottle electron energy analyzer was ~35 meV at an EKE of ~1 eV. The apparatus has been described in the detail elsewhere.[20]

The anions, ZrO_2^- and HfO_2^-, were generated by a laser vaporization source by focusing the pulsed (10 Hz), second harmonic (532 nm) beam of a Nd:YAG laser onto a zirconium rod (6.2 mm diameter, 99%, Alfa AESAR #10443) in the former case and onto a hafnium rod (5.0 mm diameter, 97%, Goodfellow HF007910) in the latter case. In both cases, the target rod was continuously rotated and translated so that the laser struck a different spot each time it was fired. The carrier gas used in the laser vaporization source was highly purified helium, which issued through a pulsed valve, having a backing pressure of ~4 atm. Oxygen was not added to the carrier gas, because the oxygen on the surface of the zirconium and hafnium rods was found to be adequate for making the metal oxide anions of interest.

Franck−Condon analyses were conducted on both the ZrO_2/ZrO_2^- and the HfO_2/HfO_2^- systems using the PESCAL program.[21]

Theoretical Methods. Initial calculations were performed with relativistic SBKJ pseudopotentials and basis sets[22] and the B3LYP exchange-correlation functional.[23] Advanced ab initio calculations were further carried out using the coupled cluster method with single, double, and noniterative triple excitations (CCSD(T)).[24] All electrons were treated on oxygens with aug-cc-pVTZ basis sets.[25] Stuttgart energy-consistent, small-core pseudopotentials and the (8s7p6d)/[6s5p3d] basis sets were used for Zr and Hf.[26] As the excess electron in the anions are localized at the metal centers, the (8s7p6d)/[6s5p3d] basis sets of Zr and Hf were further expanded with polarization and diffuse functions as described below. A small basis set (denoted as S) on M (M = Zr, Hf) included a set of diffuse d functions $\zeta(M,d) = 0.01$ and a large basis set (denoted as L) included two f and one g polarization functions[27] and two diffuse s and two diffuse d functions. The exponents of s and d diffuse functions were obtained from even-tempered progressions with a constant of 0.5, initiated from the most diffuse s and d functions in the original (8s7p6d)/[6s5p3d] basis set. The scalar relativistic effects were taken into account via the relativistic pseudopotentials obtained from Wood−Boring all-electron calculations on the atoms.[26] Spin−orbit coupling effects might be important for the hafnium compounds but they were neglected in the current approach. The CCSD(T) forces and curvatures were calculated numerically. Excited electronic states of neutral ZrO_2 and HfO_2 were calculated using time-dependent density functional theory (TDDFT) with the L basis set and the B3LYP exchange-correlation functional. The DFT calculations were performed with Gaussian98[28] and CCSD(T) calculations with MOLPRO.[29] Molden was used for the visualization of singly occupied molecular orbitals.[30]

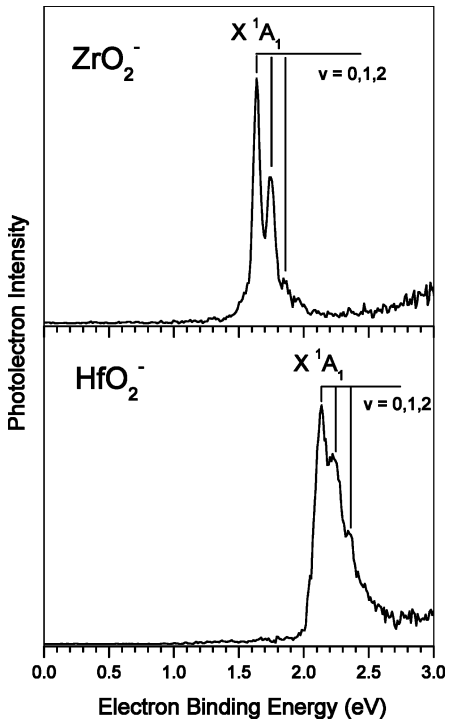

Figure 1. Photoelectron spectra of ZrO_2^- and HfO_2^- recorded with 3.493 eV photons.

Results

Experimental Results. The photoelectron spectra of ZrO_2^- and HfO_2^- are presented in Figure 1. They were both recorded with 3.493 eV photons, the third harmonic of Nd:YAG laser. Because Zr and Hf each have several isotopes, we recorded these

spectra on mass peaks, $^{90}ZrO_2^-$ and $^{176}HfO_2^-$ to avoid the possibility of contamination from nearby ZrO_2H^- and HfO_2H^-. The electron binding energies (EBE) in both spectra were calibrated against the atomic lines of the copper anion, and the uncertainty of the calibration is ±0.03 eV. The spectrum of ZrO_2^- is consistent with our former low resolution result.[31] The spectrum of ZrO_2^- exhibits a main peak at EBE = 1.64 eV, corresponding to the transition from $v = 0$ of the ground state of ZrO_2^- anion to $v = 0$ of the ground state of ZrO_2 neutral. This implies that the adiabatic electron affinity (AEA) of ZrO_2 is 1.64 ± 0.03 eV. The peaks at EBE = 1.75 and 1.86 eV correspond to excited vibrations ($v = 1$ and 2, respectively) in the electronic ground state of neutral ZrO_2. The energy spacings between adjacent peaks are both 0.11 ± 0.005 eV, corresponding to a vibrational frequency of 887 ± 40 cm^{-1} for ZrO_2. This value is consistent with that of 884.3 cm^{-1} obtained for the symmetrical stretching mode (v_1) of ZrO_2 in matrix infrared spectroscopy experiments;[13] see Table 1. In analogous fashion, the photoelectron spectrum of HfO_2^- exhibits a main peak at EBE = 2.14 eV, corresponding to the transition from $v = 0$ of the ground state of HfO_2^- anion to $v = 0$ of the ground state of HfO_2 neutral. This implies that the AEA of HfO_2 is 2.14 ± 0.03 eV. The peaks at EBE = 2.25 and 2.36 eV correspond to excited vibrations ($v = 1$ and 2, respectively) in the electronic ground state of neutral HfO_2. Again, the energy spacings between adjacent peaks are both 0.11 ± 0.005 eV, corresponding to a vibrational frequency of 887 ± 40 cm^{-1} for HfO_2. This value is also consistent with that of 883.4 cm^{-1} obtained for the symmetrical stretching mode (v_1) of HfO_2 in matrix infrared spectroscopy experiments;[13] see Table 1. We should mention that the uncertainties of v_1 frequencies obtained from the photoelectron spectra are larger than those from the matrix infrared spectra.[13]

Franck−Condon analyses were conducted on both the ZrO_2/ZrO_2^- and the HfO_2/HfO_2^- systems and the results fitted to their respective photoelectron spectra. For the ZrO_2^- photoelectron spectrum, our best fit was obtained when the symmetric stretch (v_1) of neutral ZrO_2 equaled 871 cm^{-1} and when the AEA of ZrO_2 equaled 1.65 eV. Both of these values are consistent with our a priori assignment of the ZrO_2^- photoelectron spectrum. For the HfO_2^- photoelectron spectrum, our best fit was obtained when the symmetric stretch (v_1) of neutral HfO_2 equaled 872 cm^{-1} and when the AEA of HfO_2 equaled 2.15 eV. Both of these values are again consistent with our a priori assignment of the HfO_2^- photoelectron spectrum. For both systems, the measured values of AEA and the v_1 frequencies are in excellent agreement with the calculated values, vide infra and Table 2.

Theoretical Results. The most stable structures of ZrO_2 and HfO_2 in the ground electronic states have C_{2v} symmetry. These are closed-shell systems; thus the symmetry is $^1A_1$. The structures of anionic ZrO_2 and HfO_2 maintain the C_{2v} symmetry and the excess electron occupies a fully symmetric orbital (a_1); see Figure 2. Thus the symmetry of the open-shell electronic anionic states is $^2A_1$. The calculated bond lengths, OMO bond angles, adiabatic electron affinities, and harmonic vibration frequencies for ZrO_2 and HfO_2 are listed in Table 2. The reported values AEA include vibrational zero-point energy contributions. The CCSD(T)/L values of AEA are 1.62 and 2.05 eV for ZrO_2 and HfO_2, respectively, thus in excellent agreement with the corresponding measured values of 1.64 ± 0.03 and 2.14 ± 0.03 eV. There are only small differences in the values of AEA obtained with the S and L basis sets. Including spin−orbit coupling effects may further improve the agreement with experiment for the Hf systems. The B3LYP values of AEA are overestimated with respect to the CCSD(T) results by 0.2−0.3 eV, which is typical for this exchange-correlation functional.[32,33]

TABLE 2: Calculated M−O Bond Lengths (Å), OMO Bond Angles (deg), Adiabatic Electron Affinities (eV), and Vibrational Frequencies (cm^{-1}) for ZrO_2 and HfO_2*

system	method	M−O	∠OMO	AEA	v_1	v_2	v_3
ZrO_2	CCSD(T)/L	1.797	109.6	1.62	887	281	835
	CCSD(T)/S	1.816	109.4	1.67	876	272	842
	B3LYP/SBKJ	1.806	108.0	1.85	906	295	854
ZrO_2^-	CCSD(T)/L	1.833	111.7	-	839	266	785
	CCSD(T)/S	1.853	111.9	-	829	255	790
	B3LYP/SBKJ	1.843	110.3	-	850	272	799
HfO_2	CCSD(T)/L	1.815	109.9	2.05	869	266	801
	CCSD(T)/S	1.826	109.8	2.07	859	254	805
	B3LYP/SBKJ	1.797	107.3	2.32	898	293	821
HfO_2^-	CCSD(T)/L	1.855	114.3	-	819	242	752
	CCSD(T)/S	1.867	115.1	-	808	224	753
	B3LYP/SBKJ	1.833	111.6	-	844	255	772

[a] The values of AEA include vibrational zero-point energy corrections. v_1 is the symmetric stretching mode, v_2 is the bending mode, and v_3 is the asymmetric stretching mode. "L" and "S" stand for the "large" and "small" basis sets, see text. For "SBKJ", see ref 22.

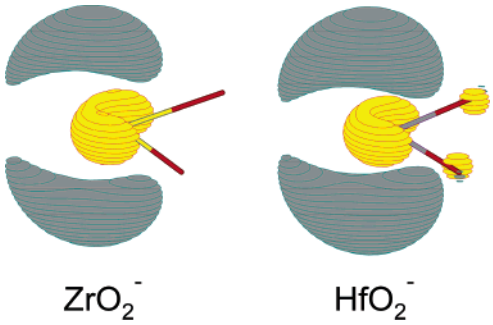

Figure 2. Excess electron in MO_2^- (M = Zr, Hf) occupying an a_1-symmetry orbital dominated by the M's *n*s and (*n* − 1)d orbitals.

Our calculations confirm that the neutral ZrO_2 and HfO_2 have C_{2v} symmetry and a very similar bond length and ∠OMO.[14,15] The M−O distances calculated at the CCSD(T)/L level are 1.797 Å for ZrO_2 and 1.815 Å for HfO_2, thus ca. 0.03−0.04 Å longer than the microwave spectroscopy predictions.[14,15] The bond lengths are sensitive to the selection of one-electron basis set (L vs S) and the computational method (CCSD(T) vs B3LYP). The CCSD(T)/L values of ∠OMO of 109.6° and 109.9° are in excellent agreement with the previous findings of 108.11 ± 0.08° and 107.51 ± 0.01° for ZrO_2[14] and HfO_2,[15] respectively.

The calculated, harmonic, CCSD(T)/L frequencies for the symmetrical stretching mode of 887 cm^{-1} (ZrO_2) and 869 cm^{-1} (HfO_2) are consistent with the 887 ± 40 cm^{-1} value resulting from the photoelectron spectra. However, the more accurate results from matrix infrared measurements[13] of 884.3 cm^{-1} (ZrO_2) and 883.4 cm^{-1} (HfO_2) reveal that the calculated values might be inaccurate by ca. 15−20 cm^{-1}. The calculated harmonic CCSD(T)/L frequencies for the asymmetrical stretching mode are also inaccurate by ca. 20 cm^{-1}. The calculated frequency for the bending mode of ZrO_2 (281 cm^{-1}) agrees well with the 290 cm^{-1} value determined from the inertial defect.[14] The B3LYP vibrational force constants are systematically larger for ZrO_2 than for HfO_2 and so are the reduced masses resulting in very similar values of vibrational frequencies for the two molecules.

Upon the excess electron attachment the M−O bond lengths increase by ca. 0.04 Å and ∠OMO's increase by 2−4°; see Table 2. The differences in geometries between the neutral and the anion are along the symmetrical stretching mode, v_1, and

the bending mode, υ_2. The frequencies of all vibrational modes decrease upon the excess electron attachment with a larger shift (30−50 cm^{-1}) for the stretching modes and a smaller shift of 15−25 cm^{-1} for the bending mode.

ZrO_2 and HfO_2 are polar molecules with the experimentally measured dipole moments of 7.80[14] and 7.92[15] D, respectively. The calculated dipole moments are consistent with experiment in predicting a larger polarity of HfO_2 than of ZrO_2, but the absolute values of dipole moments are overestimated. Indeed, the corresponding B3LYP/S values are 8.00 and 8.06 D. The overestimation is even larger at the CCSD/S level with the corresponding values being 8.40 and 8.60 D. The effective charge on the metal, determined from the Mulliken population analysis with the B3LYP/SBKJ wave functions, is +1.15 and +1.10 e, for HfO_2 and ZrO_2, respectively. The excess electron is found to localize on the metal atom, where the positive pole of the dipole is (Figure 2). An excess electron bound by a polar molecule, which does not contain a transition metal atom, is typically described by a fully symmetric sp-type hybrid orbital; see ref 34 for numerous examples. In the case of ZrO_2 and HfO_2, however, the *n*s and (n − 1)d orbitals are available on the metal atom, whereas the *n*p orbitals are higher in energy. The excess electron is then described by a fully symmetric sd-type hybrid orbital with a_1 symmetry (Figure 2).

The low lying electronic states of the neutral ZrO_2 and HfO_2 were characterized at the TDDFT/B3LYP/S level of theory. For both systems, the lowest excited singlet and triplet states are of B_1 symmetry, with the b_1 orbital localized on the metal atom. The more stable $^3B_1$ states are at 2.15 and 1.55 eV with respect to the ground singlet state for ZrO_2 and HfO_2, respectively. The related $^1B_1$ states are less stable by 0.07−0.08 eV. Thus the excited electronic states of the neutral do not contribute to the photoelectron spectra recorded with the 3.493 eV photons.

Discussion

The significant electron affinity difference between ZrO_2 and HfO_2, combined with the lack of a measurable difference in their υ_1 vibrational frequencies and very similar molecular geometries, appears to indicate electronic structure rather than size or bonding effects as the primary basis for reactivity and stability differences between ZrO_2 and HfO_2. The difference in stability of the ZrO_2/Si and HfO_2/Si interfaces with respect to formation of metal silicides was interpreted in terms of a larger stability of (i) HfO_2 than ZrO_2 and (ii) zirconium rather than hafnium silicides.[18] The current results shed new light on differences in electronic structure of ZrO_2 and HfO_2.

Recent computational results on various polymorphs of HfO_2 and ZrO_2 indicate that the former is more ionic than the latter.[35] The former also has a larger band gap across all polymorphs. These results are consistent with the finding that the calculated heat of formation for the monoclinic phase is larger by 0.60 eV/formula unit for HfO_2 than for ZrO_2, with the experimental difference being 0.49 eV.[17] The difference in ionicity is also confirmed by dipole moments of HfO_2 and ZrO_2, 7.92 and 7.80 D, respectively.[15,14] A difference in the dipole moment might contribute to the different values of AEA for HfO_2 and ZrO_2; see Tables 1 and 2 and Figure 1. All these findings are consistent with a small difference in the electronegativity of Zr and Hf: 1.4 and 1.3, respectively, according to Pauling's scale.[36]

How important is the lanthanide contraction for Hf? It has recently been demonstrated for various polymorphs of MO_2 that the volume per formula unit is smaller for HfO_2 than for ZrO_2, as if the ionic radius was smaller for "Hf(+4)" than for "(Zr-(+4)".[35] The difference was 3.9% for the most stable monoclinic phase. This result is surprising because usually for congeneric elements an increase in the atomic number leads to an increase of the atomic or ionic radius. For typical elements from the second and third transition metal rows such an increase is reduced by the electron occupation of the 4f and relativistic effects, whereas for Zr and Hf the relative sizes are apparently reversed, as in the case of monovalent coin metals.[37] Indeed, the recommended ionic radius for "Hf(+4)" is smaller by 0.01 Å than that for "Zr(+4)",[12] which qualitatively confirms the structural predictions for bulk phases. For the molecular systems, however, the measured M−O distance is larger for ZrO_2 (1.7710 ± 0.0007 Å)[14] than for HfO_2 (1.7764 ± 0.0004 Å).[15] Clearly, the parallelism between structural properties of bulk phases and molecular systems is limited.

The neutral ZrO_2 and HfO_2 are highly polar and the excess electron is described by a sd-type hybrid orbital localized on the metal atom. In the case of HfO_2^- small amplitudes can be also identified on oxygens (Figure 2). The availability of (n − 1)d orbitals makes the charge distribution of an excess electron different than in anions of polar molecules that do not contain a transition metal atom. One might only speculate what the charge distribution of an excess electron would be in polar molecules with available (n − 2)f orbitals, such as CeO_2 or BaO anions.

Because Ti, Zr, and Hf are all in the same group of the periodic table, it is also interesting to compare the electron affinities and vibrational frequencies of ZrO_2 and HfO_2 with those of TiO_2. Wu and Wang[38] reported the photoelectron spectrum of TiO_2^-. They found the adiabatic electron affinity of TiO_2 to be 1.59 ± 0.03 eV and the frequency of υ_1 to be 940 ± 40 cm^{-1}. These properties of TiO_2, HfO_2, and ZrO_2 are compared in Table 1. Note that ZrO_2 and HfO_2 have essentially identical vibrational frequencies, whereas the υ_1 vibrational frequency of TiO_2 differs from them. This indicates differences in bonding strength and reduced masses between TiO_2 and ZrO_2 (HfO_2). Consistent with this, the atomic and ionic radii of zirconium and hafnium are the same to within 0.01 Å, whereas the ionic radius of Ti(+4) is smaller by 0.1 Å than those of Zr(+4) and Hf(+4).[12] The comparison reverses, however, when adiabatic electron affinities are compared. The electron affinities of TiO_2 and ZrO_2 are rather similar, differing by only 0.05 eV, whereas the electron affinities of HfO_2 and ZrO_2 differ substantially, i.e., by 0.50 eV. These comparisons reinforce the implication that differences in the electronic structures of Hf and Zr are at the root of chemical differences between ZrO_2 and HfO_2. This points to the nonnegligible role of f-electrons and relativistic effects in the chemistry of hafnium compounds.

It may be useful to mention that there are other examples among atomic metals, metal−ligand complexes, and metal dimer and cluster anions, in which the excess electron occupies a metal s orbital, which likewise shows an increased electron affinity for the third transition series congener, mirroring the trend observed here.[39] This pattern has been ascribed to relativistic effects, resulting in more strongly bound s electrons in the third transition series. Because the orbital occupied by the extra electron in ZrO_2^- and HfO_2^- has a significant metal s character (Figure 2), the reported values of AEA are consistent with this trend. This observation supports our conclusions that the presence of f electrons in the third transition series affects valence electronic structure controlled by the 5d and 6s orbitals.

Acknowledgment. We acknowledge the reviewers for their insightful and constructive comments. K.B.'s portion of this work was supported by The Division of Materials Science and Engineering, Office of Basic Energy Sciences, U.S. Department

of Energy under Grant No. DE-FG0295ER45538. Acknowledgment is also made to the donors of the Petroleum Research Fund, administered by the American Chemical Society, for partial support of this research under grant No. 28452-AC6. M.G.'s and J.L.'s portion of this work was supported by DOE Basic Energy Sciences, Division of Chemical Sciences. I.D. is a holder of a Foundation for Polish Science (FNP) Award. Computing resources were available through (i) a Computational Grand Challenge Application grant from the Molecular Sciences Computing Facility (MSCF) in the Environmental Molecular Sciences Laboratory, a national scientific user facility sponsored by the U.S. DOE, OBER and located at PNNL, and (ii) the National Energy Research Scientific Computing Center (NERSC). PNNL is operated by Battelle for the U.S. DOE under Contract DE-AC06-76RLO 1830.

References and Notes

(1) Copel, M.; Gribelyuk, M.; Gusev, E. *Appl. Phys. Lett.* **2000**, *76*, 436.

(2) Wilk, G. D.; Wallace, R. M.; Anthony, J. M. *J. Appl. Phys.* **2001**, *89*, 5243 and references therein.

(3) Jeon, T. S.; White, J. M.; Kwong, D. L. *Appl. Phys. Lett.* **2001**, *78*, 368.

(4) Robertson, J. *J. Vac. Sci. Technol. B* **2000**, *18*, 1785.

(5) Yang, X.; Jentoft, F. C.; Jentoft, R. E.; Girgsdies, F.; Ressler, T. *Catal. Lett.* **2002**, *81* (1−2), 25.

(6) Rossi, S. De.; Ferraris, G.; Valigi, M.; Gazzoli, D. *Appl. Catal. A-Gen.* **2002**, *231* (1−2), 173.

(7) Mulas, G.; Deledda, S.; Monagheddu, M.; Cocco, G.; Cutrufello, M. G.; Ferino, I.; Solinas, V. *Metastable, Mechanically Alloyed and Nanocrystalline Materials*; 2000; Vol. 343, p 889.

(8) Andrievsky, E. R.; Redko, V. P.; Lopato, L. M. Euro Ceramics VII, **2002**, *206* (2), 1113.

(9) Hastie, J. W.; Bonnell, D. W.; Schenck, P. K. *J. Nucl. Mater.* **2001**, *294* (1−2), 175.

(10) Sasakim, H. *J. Eur. Ceram. Soc.* **1995**, *15* (4), 329.

(11) Andrews, M. J.; Ferber, M. K.; Lara-Curzio, E. *J. Eur. Ceram. Soc.* **2002**, *22* (14−15), 2633.

(12) Cotton, F. A.; Wilkinson, G.; Murillo, C. A. Bochmann, M. *Advanced Inorganic Chemistry*; John Wiley & Sons: New York, 2000.

(13) Chertihin, G. V.; Andrews, L. *J. Phys. Chem.* **1995**, *99*, 6356.

(14) Brugh, D. J.; Suenram, R. D.; Stevens, W. J. *J. Chem. Phys.* **1999**, *111*, 3526.

(15) Lesarri, A.; Suenram, R. D.; Brugh, D. *J. Chem. Phys.* **2002**, *117*, 9651.

(16) Lowther, J. E. *Mater. Res. Bull.* **2003**, *28*, 189.

(17) Barin, I. *Thermochemical Data of Pure Substances*, 3rd ed.; VCH: Wienheim, 1995; Vol. I and Vol. II.

(18) Gutowski, M.; Jaffe, J. E.; Liu, C.-L.; Stoker, M.; Hegde, R. I.; Rai, R. S.; Tobin, P. J. *Appl. Phys. Lett.* **2002**, *80*, 1897.

(19) Kaufman, M.; Muenter, J.; Klemperer, W. *J. Chem. Phys.* **1967**, *47*, 3365.

(20) Thomas, O. C.; Zheng, W.; Bowen, K. H. *J. Chem. Phys.* **2001**, *114*, 551.

(21) Ervin, K. M.; Ramond, T. M.; Davico, G. E.; Schwartz, R. L.; Casey, S. M.; Lineberger, W. C. *J. Phys. Chem. A* **2001**, *105*, 10822. K. M. Ervin, PESCAL, Fortran program, 2004.

(22) Stevens, W. J.; Basch, H.; Krauss, M. *J. Chem. Phys.* **1984**, *81*, 6026. Stevens, W. J.; Krauss, M.; Basch, H.; Jasien, P. G. *Can. J. Chem.* **1992**, *70*, 612.

(23) Becke, A. D. *Phys. Rev. A* **1988**, *38*, 3098. Becke, A. D. *J. Chem. Phys.* **1993**, *98*, 5648. Lee, C.; Yang, W.; Paar, R. G. *Phys. Rev. B* **1988**, *37*, 785.

(24) Taylor, P. R. In *Lecture Notes in Quantum Chemistry II*; Roos, B. O., Ed.; Springer-Verlag: Berlin, 1994.

(25) Kendall, R. A.; Dunning, T. H., Jr.; Harrison, R. J. *J. Chem. Phys.* **1992**, *96*, 6796.

(26) Andrae, D.; Haeussermann, U.; Dolg, M.; Stoll, H.; Preuss, H. *Theor. Chim. Acta* **1990**, *77*, 123.

(27) Martin, J. M. L.; Sundermann, A. *J. Chem. Phys.* **2001**, *114*, 3408.

(28) Frisch, M. J.; Trucks, G. W.; Schlegel, H. B.; Scuseria, G. E.; Robb, M. A.; Cheeseman, J. R.; Zakrzewski, V. G.; Montgomery, J. A., Jr.; Stratmann, R. E.; Burant, J. C.; Dapprich, S.; Millam, J. M.; Daniels, A. D.; Kudin, K. N.; Strain, M. C.; Farkas, O.; Tomasi, J.; Barone, V.; Cossi, M.; Cammi, R.; Mennucci, B.; Pomelli, C.; Adamo, C.; Clifford, S.; Ochterski, J.; Petersson, G. A.; Ayala, P. Y.; Cui, Q.; Morokuma, K.; Malick, D. K.; Rabuck, A. D.; Raghavachari, K.; Foresman, J. B.; Cioslowski, J.; Ortiz, J. V.; Stefanov, B. B.; Liu, G.; Liashenko, A.; Piskorz, P.; Komaromi, I.; Gomperts, R.; Martin, R. L.; Fox, D. J.; Keith, T.; Al-Laham, M. A.; Peng, C. Y.; Nanayakkara, A.; Gonzalez, C.; Challacombe, M.; Gill, P. M. W.; Johnson, B. G.; Chen, W.; Wong, M. W.; Andres, J. L.; Head-Gordon, M.; Replogle, E. S.; Pople, J. A. *Gaussian 98*, revision A.11; Gaussian, Inc.: Pittsburgh, PA, 1998.

(29) MOLPRO is a package of ab initio programs written by H.-J. Werner, P. J. Knowles, M. Schütz, R. Lindh, P. Celani, T. Korona, G. Rauhut, F. R. Manby, R. D. Amos, A. Bernhardsson, A. Berning, D. L. Cooper, M. J. O. Deegan, A. J. Dobbyn, F. Eckert, C. Hampel, G. Hetzer, A. W. Lloyd, S. J. McNicholas, W. Meyer, M. E. Mura, A. Nicklass, P. Palmieri, R. Pitzer, U. Schumann, H. Stoll, A. J. Stone R. Tarroni, and T. Thorsteinsson.

(30) Schaftenaar, G.; Noordik, J. H. *J. Comput.-Aided Mol. Design* **2000**, *14*, 123.

(31) Thomas, O. C.; Xu, S.-J.; Lippa, T. P.; Bowen, K. H. *J. Cluster Sci.* **1999**, *10*, 525.

(32) Rak, J.; Skurski, P.; Gutowski, M. *J. Chem. Phys.* **2001**, *114*, 10673.

(33) Gutowski, M.; Dabkowska, I.; Rak, J.; Xu, S.; Nilles, J. M.; Radisic, D. K.; Bowen, H. *Eur. Phys. J. D* **2002**, *20*, 431.

(34) Gutowski, M.; Skurski, P.; Boldyrev, A. I.; Simons, J.; Jordan, K. D. *Phys. Rev. A* **1996**, *54*, 1906. Gutowski, M.; Jordan, K. D.; Skurski, P. *J. Phys. Chem. A* **1998**, *102*, 2624. Gutowski, M.; Hall, C.; Adamowicz, L.; Hendricks, J. H.; de Clercq, H. L.; Lyapustina, S. A.; Nilles, J. M.; Xu, S. J.; Bowen, K. H., Jr. *Phys. Rev. Lett.* **2002**, *88*, 143001. Gutowski, M.; Skurski, P. *Chem. Phys. Lett.* **1999**, *303*, 65.

(35) Jaffe, J. E.; Bachorz, R. A.; Gutowski, M. *Phys. Rev. B* **2005**, *72*, 144107.

(36) Pauling, L. *The Nature of the Chemical Bond*, 3rd ed.; Cornell University Press: Ithaca, NY, 1960.

(37) Liao, M. S.; Schwarz, W. H. E. *Acta Crystallogr.* **1994**, *B50*, 9.

(38) Wu, H. B.; Wang, L.-S. *J. Chem. Phys.* **1997**, *107*, 8221.

(39) Bengali, A. A.; Casey, S. M.; Cheng, C−L.; Dick, J. P.; Fenn, P. T.; Villalta, P. W.; Leopold, D. G. *J. Am. Chem. Soc.* **1992**, *114*, 5257.